PCCP

The second virial coefficient of the dipolar two center Lennard-Jones model†

Carlos Vega, Carl McBride and Carlos Menduiña

Departamento de Química Física, Facultad de Ciencias Químicas, Universidad Complutense de Madrid, Ciudad Universitaria, 28040, Madrid, Spain. E-mail: carlos@ender.quim.ucm.es

Received 24th January 2002, Accepted 26th February 2002
First published as an Advance Article on the web 20th May 2002

The second virial coefficients of two-center Lennard-Jones molecules which contain an embedded point dipole have been determined *via* numerical integration. A number of models with different reduced bond lengths and dipole moments have been considered. For each model the second virial coefficient has been calculated for a number of temperatures. It is shown that the presence of the dipole moment significantly raises the Boyle temperature and, for a given temperature, reduces the value of the second virial coefficient with respect to the non-polar model. It is shown that the model can describe correctly the second virial coefficient of some refrigerants.

I. Introduction

The equation of state of a low density gas can be described by the virial expansion. The virial expansion expresses the compressibility factor as a function of density, with temperature dependent coefficients known as virial coefficients. Both the second and the third virial coefficients can be measured experimentally[1–5] for both pure fluids and their mixtures. The second virial coefficient provides information concerning the intermolecular forces between a pair of molecules. Similarly the third virial coefficient provides information about the intermolecular forces between three molecules, *etc.* In the nineteen thirties and forties it was shown that the virial coefficients may also be calculated if the intermolecular forces between molecules are known.[6–11] Second, third, and fourth virial coefficients can be computed by evaluating integrals involving two, three and four molecules respectively. The expression for the second virial coefficient B_2 is especially simple, being given by minus one half of the integral of the angle-averaged Mayer function over all possible values of the distance between the centers of mass (*i.e.* reference points) of the two molecules. For molecules which have spherical symmetry, the second virial coefficient can be easily computed, either analytically[12,13] or numerically. When the molecule is non-spherical then one must compute the second virial coefficient numerically, although in some select cases it may be computed analytically, for instance in the case of hard convex bodies[14] or their Kihara counterparts.[15,16]

One of the most popular models used to describe the interaction energy between non-spherical molecules is the interaction site model (ISM).[11] In this model atoms or groups of atoms in the molecule are replaced by Lennard-Jones interactions sites. Probably one of the simplest ISM is the two center Lennard-Jones model (from here on denoted as the 2CLJ model). In this model the molecule is described by two Lennard-Jones (LJ) sites (with parameters ε and σ) whose centers are separated by a distance L. This model can be used to represent diatomic molecules, such as N_2, O_2, F_2, Cl_2 *etc*. Determination of B_2 for 2CLJ models was first performed by Maitland *et al.* twenty years ago[17] and more recently by Boublik.[18]

The 2CLJ is an interesting model, although it lacks one important feature: a multipole moment. In a recent study[19] the second virial coefficients of 2CLJ models which have an embedded ideal quadrupole moment (2CLJQ) were evaluated. In the study a number of molecular elongations (defined by the reduced bond length $L^* = L/\sigma$) and values of the reduced quadrupole moment $(Q^*)^2 = Q^2/(\varepsilon\sigma^5)$ were considered. The effect of the quadrupole moment on the Boyle temperature T_B and on B_2 and the possibility of describing real substances using the 2CLJQ model was discussed. In a similar manner this work treats a 2CLJ model which contains an embedded ideal dipole moment. The model consists of two identical LJ sites separated by a distance L with an ideal dipole moment located at the center of mass of the molecule. We shall denote this model as the 2CLJD model. The 2CLJD model represents a logical extension to the Stockmayer[20] potential which consists of one LJ site plus an ideal dipole moment. The Stockmayer potential has proven to be useful in describing the second[21–24] and third virial coefficients[25] of dipolar substances. In this work the second virial coefficient as a function of the temperature has been numerically calculated for several 2CLJD models. This model is of interest from two points of view; from a fundamental perspective it provides a better understanding of the effect that the dipole moment has on the second virial coefficient, and from a practical point of view it may be used to describe the second virial coefficient of real substances.

We shall consider the case of a dipole moment that is aligned with the molecular axis as well as the case where the dipole moment forms an angle, α, with the molecular axis. To the best of our knowledge the only previous calculations of B_2 for 2CLJD molecules are those by Vega *et al.*[26] for the refrigerant molecule CH_3CHF_2 (R152a), and those of Kohler and van Nhu.[27]

A number of remarks should be made concerning the use of the 2CLJD model to describe real substances. Firstly, given that the model has no polarisability then dipole-induced dipole effects are non existent. Due to this we should see a small difference (of the order of 5%) in the interaction potential for the 2CLJD model when compared to 'real molecules' having anisotropic polarisabilities. Secondly, in the model described here

† Electronic supplementary information (ESI) available: computer programs and ancillary data. See http://www.rsc.org/suppdata/cp/b2/b200781a/

 DOI: 10.1039/b200781a

use is made of an ideal, point like, dipole rather than a charge distribution. Values for B_2 will be noticeably different for point like dipole model and a model with a charge distribution. Finally, in this study, the Lennard-Jones sites are of equal size. However, real diatomic molecules that have a dipole moment are formed by two distinct atoms. Thus HCl has a dipole moment whereas N_2 does not; the bonding of two identical atoms or groups can not lead to the existence of a dipole moment in the molecule. In view of this the 2CLJD model with two identical LJ sites does not seem to be the best candidate to describe a real dipolar diatomic molecule. The Stockmayer potential also suffers from this unrealistic aspect; *i.e.* a spherical molecule cannot have a dipole moment. This is not to say that a model could not be devised that has a spherical aspect whilst having an anisotropic charge distribution.

Having said this the study of the 2CLJD is interesting for two reasons. Firstly by comparing the results of the 2CLJ, 2CLJQ and 2CLJD models one can assess the influence of a quadrupole or a dipole moment on the second virial coefficient, since the dispersion forces are exactly the same in the three models. Any differences can be attributed to the presence of polar forces. A second justification for the study of the 2CLJD model is the ability to explore the parameter space of the model. The second virial coefficient of the 2CLJD model depends on the reduced temperature $T^* = T/(\varepsilon/k)$, the reduced bond length L^*, the reduced dipole moment $(\mu^*)^2$ and the angle formed by the dipole moment with the molecular axis α. In this work we have explored the dependence of B_2 on these four independent variables. This is probably the limiting number of independent variables for which a comprehensive study can be readily performed. In total the number of models considered in this work amounts to 11 different elongations, 8 values of the dipole moment and 4 different angles, resulting in 352 different models having been considered. For each of these 352 models approximately 300 different temperatures were considered. For a heteronuclear diatomic 2CLJD model, there would be three additional independent variables, namely the ratio between σ of the two LJ sites, the ratio between the ε values of the two independent sites and the direction (from the smaller to the larger or from the larger to the smaller atom) of the dipole moment. Therefore a comprehensive study of heteronuclear 2CLJD models is out of the question. Of course this is not to say that one cannot easily compute B_2 for a particular heteronuclear model.

The scheme of the paper is as follows. In Section II details of the model and the calculation of B_2 are given. In Section III, results for B_2 and T_B for different 2CLJD models are presented. Finally in Section IV we apply our results for the 2CLJD to the description of B_2 of real substances.

II. Model and calculation details

In this work molecules are described by a two center Lennard-Jones model (2CLJ). The two sites are identical and are located at a distance L. The parameters controlling the Lennard-Jones interaction (LJ) are σ and ε. A point dipole is located at the center of mass of the molecule. We shall denote this model as the two center Lennard-Jones dipolar model (2CLJD). The model is described by two reduced quantities, namely, the reduced bond length $L^* = L/\sigma$ and the reduced dipole moment $(\mu^*)^2$ which is given by

$$(\mu^*)^2 = \frac{\mu^2}{\varepsilon\sigma^3}. \tag{1}$$

The pair interaction between a pair of molecules is given by:

$$u(1,2) = \sum_{i=1}^{2}\sum_{j=1}^{2} u_{ij}^{\mathrm{LJ}} + u_{\mathrm{DD}} \tag{2}$$

where u_{ij}^{LJ} and u_{DD} are given by:

$$u_{ij}^{\mathrm{LJ}} = 4\varepsilon\left(\left(\frac{\sigma}{r_{ij}}\right)^{12} - \left(\frac{\sigma}{r_{ij}}\right)^{6}\right) \tag{3}$$

$$u_{\mathrm{DD}}/\varepsilon = \frac{(\mu^*)^2}{(r^*)^3}(s_1 s_2 c_{12} - 2c_1 c_2) \tag{4}$$

where r_{ij} is the distance between site i of molecule 1 and site j of molecule 2, $r^* = r/\sigma$ is the reduced distance between the centers of mass of the molecule. We also have $c_i = \cos(\theta_i)$, $s_i = \sin(\theta_i)$ and $c_{12} = \cos(\phi_2 - \phi_1)$. θ_1, θ_2 and ϕ_1 are illustrated in Fig. 1. Notice that the dipole moment is a vector. The angle formed by the dipole moment with the molecular axis is represented by α. The reduced second virial coefficient $B_2^* = B_2/\sigma^3$ has been computed as a function of the reduced temperature $T^* = T/(\varepsilon/k)$ for a number of linear models. We have considered models with $L^* = 0$, 0.1, 0.2, 0.3, 0.4, 0.5, 0.6, 0.7, 0.8, 0.9, 1 and with $(\mu^*)^2 = 0$, 1, 2, 3, 4, 6, 8, 10. For each of the models the following values of α were considered $\alpha = 0$, 30, 60, 90°. The case $\alpha = 0$ corresponds to the situation where the dipole moment is aligned with the molecular axis, whereas the case $\alpha = 90$ corresponds to the case where the dipole moment is orthogonal to the molecular axis. The total number of models considered is $11 \times 8 \times 4 = 352$.

The value of the second virial coefficient of a pair of molecules can be obtained by evaluating the following expression:

$$B_2 = -\frac{1}{2}\int (\langle \exp(-\beta u)\rangle - 1) 4\pi r^2 \, \mathrm{d}r \tag{5}$$

where $\beta = 1/(kT)$, r is the distance between the center of mass of two molecules and $\langle \exp(-\beta\, u)\rangle$ is the orientational average of the Boltzmann factor between two molecules for a fixed value of r. Obviously the complexity of the calculation of B_2 for a non-spherical molecule arises in the determination of $\langle \exp(-\beta\, u)\rangle$. In this work $\langle \exp(-\beta\, u)\rangle$ was evaluated for each value of r using Conroy's integration method.[28] We follow Nezbeda *et al.*[29] and generate 76 079 relative orientations for each value of r.[29] The average $\langle \exp(-\beta\, u)\rangle$ is evaluated for 451 different values of r (from $r = 0$ up to $r = 20\sigma$). Finally the integral of eqn. (5) is obtained by using Simpson's integration rule. We estimate the typical uncertainty of our calculations of B_2 to be of the order of 1%.

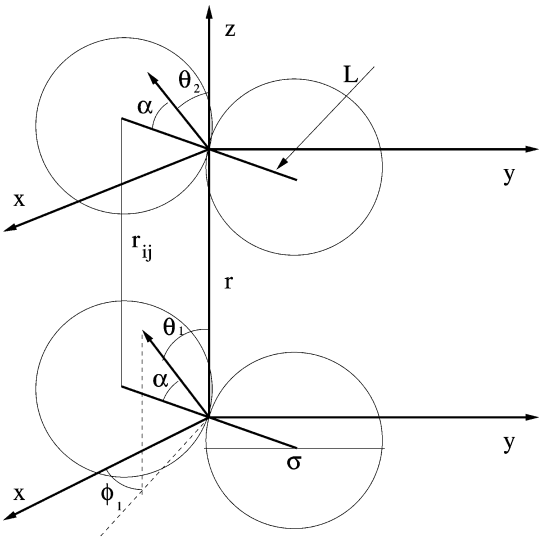

Fig. 1 Schematic diagram of the 2CLJD model used in this work. The vector representing the dipole moment forms an angle α with the molecular axis.

For each model B_2 has been evaluated for about 300 different temperatures. The temperatures were chosen so that the largest temperature is slightly higher than the Boyle temperature and the lowest temperature is one for which B_2^* adopts a large negative number.

III. Results

The number of generated data points for B_2 is of the order of 100 000 and as such precludes tabular representation. In view of this the source data can be obtained directly from the authors or as electronic supplementary information (ESI).† We shall now discuss some of the results of this work. Let us start by analyzing the effect of the dipole moment on B_2. For this purpose we shall compare B_2^* for two models with the same elongation but having different dipole moments. In Fig. 2 results are shown for two models with the same anisotropy (*i.e.* $L^* = 0.5$) but with different dipole moments (*i.e* $(\mu^*)^2 = 0$ and 6). Results are presented as a function of the reduced temperature T^*. As expected, for a given temperature the second virial coefficient is lower for the dipolar model. Notice that although the un-weighted orientational average of the dipolar potential is zero, $\langle u_{DD} \rangle = 0$,[30] this is not the case for the average of the Boltzmann factor. Therefore, the presence of the dipole increases the strength of the attractive forces in the system thus explaining the decrease in B_2 for a given temperature. For spherical dipolar and quadrupolar molecules this was shown by Keesom.[31,32] It is interesting to compare the results of the two models with $(\mu^*)^2 = 6$, for example the $\alpha = 0$ model and the $\alpha = 60$ model. As can be seen the second virial coefficient of the model with a non-zero value of α is lower than that of the model with $\alpha = 0$. This was observed previously by Vega *et al.*[26]

In addition to the second virial coefficient calculations we have also determined the Boyle temperature, T_B, of each model. The Boyle temperature is defined as the temperature at which the second virial coefficient vanishes. In Table 1 the Boyle temperature for some 2CLJD models with $\alpha = 0$ are presented, and for $\alpha = 60$ in Table 2. As can be seen T_B decreases with L^* and increases with $(\mu^*)^2$. By comparing the results of Tables 1 and 2 it can be seen that the Boyle temperature also increases with the value of α. This means that for a certain value of L^* and $(\mu^*)^2$ the second virial coefficient becomes more negative as α increases. In other words, a non-axial dipole moment is more efficient in reducing the second virial coefficient (increasing the Boyle temperature) than an axial dipole moment. The Boyle temperatures of all the models considered in this work can can be obtained as ESI.† We have fitted the reduced Boyle temperature T_B^* in the range $L^* = (0.2, 1)$ to the following empirical formula:

$$\begin{aligned} T_B^* = {} & (d_1 + d_2 L^* + d_3 L^{*2} + d_4 L^{*3} + d_5 L^{*4}) \\ & + x((f_1 + f_2 L^* + f_3 L^{*2}). \\ & + (f_4 + f_5 L^* + f_6 L^{*2})x \\ & + (f_7 + f_8 L^* + f_9 L^{*2})x^2 \\ & + (f_{10} + f_{11} L^* + f_{12} L^{*2})x^3) \\ & + \alpha x((e_1 + e_2 L^* + e_3 L^{*2} + e_4 x + e_5 x^2) \\ & + (e_6 + e_7 L^* + e_8 L^{*2} + e_9 x + e_{10} x^2)\alpha \\ & + (e_{11} + e_{12} L^* + e_{13} L^{*2} + e_{14} x + e_{15} x^2)\alpha^2 \\ & + (e_{16} + e_{17} L^* + e_{18} L^{*2} + e_{19} x + e_{20} x^2)\alpha^3) \end{aligned} \quad (6)$$

where $x = (\mu^*)^2$. Values of the coefficients d_i, f_i, and e_i are presented in Table 3. The sum of errors of the fit of eqn. (6) is

$$\frac{\sum_1^{288} \left| T_B^* - T_B^{*,\mathrm{fit}} \right|}{N_{\mathrm{points}}} = 0.02. \quad (7)$$

We shall now compare the second virial coefficient of a dipolar and a quadrupolar model with the same reduced bond length. In Fig. 3 the values of B_2 are plotted for two models with $L^* = 1$, one of them having a quadrupole moment of $(Q^*)^2 = 4$ and the other with a dipole moment $(\mu^*)^2 = 4$. As can be seen, for identical values of the reduced multipolar moment the quadrupolar model presents the smaller second virial coefficient. The quadrupole moment is more efficient than the dipole moment in reducing the second virial coefficient of a 2CLJ model at a certain temperature (given the same reduced multipole moment). The vapor–liquid equilibria of the 2CLJD model have been determined *via* Gibbs–Duhem integration simulations by Lisal *et al.*[33] The vapor–liquid equilibria for the 2CLJQ model have also been determined from the $NpT+$ test particle method by Stoll *et al.*[34] It is found that for a certain elongation the critical temperature of the quadrupolar moment is higher than that of the dipolar model when the same value of the reduced dipole moment is used. The results of Fig. 3 are consistent with this observation. Another

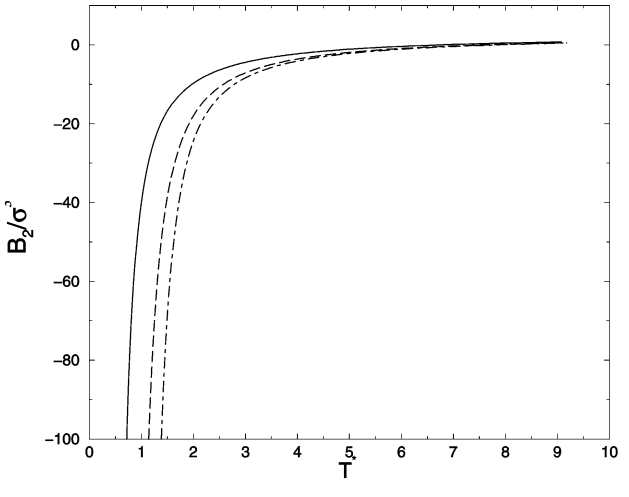

Fig. 2 Reduced second virial coefficient $B_2^* = B_2/\sigma^3$ for $L^* = 0.5$ as a function of the reduced temperature $T^* = T/(\varepsilon/k)$ for molecules with $(\mu^*)^2 = 0$ (solid line) and $(\mu^*)^2 = 6$ with $\alpha = 0$ (dashed line) and $(\mu^*)^2 = 6$ with $\alpha = 60$ (dash-dotted line).

Table 1 Reduced Boyle temperature for 2CLJD model with $\alpha = 0$. The results for $L^* = 0$ correspond to the Stockmayer potential (one LJ site with a dipole moment) as opposed to two superimposed LJ sites with a dipole moment

	$(\mu^*)^2$				
L^*	0	2	4	8	10
1	3.978	4.046	4.236	4.890	5.308
0.8	4.688	4.767	4.989	5.750	6.237
0.6	5.851	5.946	6.211	7.127	7.715
0.4	7.821	7.937	8.264	9.402	10.140
0	3.417	4.010	5.321	8.716	10.616

Table 2 Reduced Boyle temperature for 2CLJD model with $\alpha = 60$

	$(\mu^*)^2$				
L^*	0	2	4	8	10
1	3.978	4.101	4.445	5.641	6.454
0.8	4.688	4.810	5.147	6.270	6.974
0.6	5.851	5.979	6.335	7.533	8.287
0.4	7.821	7.960	8.351	9.695	10.556

Table 3 Parameters of the fit (see eqn. (6) of the main text) for the reduced Boyle temperature of 2CLJD models. This fit is valid for reduced bond lengths between 0.2 and 1, for $(\mu^*)^2$ smaller than 10 and for values of α between 0 and 90

d_1	16.05429687554756
d_2	-30.53813239991681
d_3	30.14164265332427
d_4	-14.08558417650496
d_5	2.406606047549587
f_1	-0.172327610799913
f_2	0.627540094530006
f_3	-0.493778497229557
f_4	0.145317892481520
f_5	-0.406323035035317
f_6	0.299940813391917
f_7	$-1.700872159110936 \times 10^{-2}$
f_8	$5.932041964753851 \times 10^{-2}$
f_9	$-4.611937237060716 \times 10^{-2}$
f_{10}	$7.969772314238590 \times 10^{-4}$
f_{11}	$-2.928499196763296 \times 10^{-3}$
f_{12}	$2.297075198272710 \times 10^{-3}$
e_1	$1.418043183518705 \times 10^{-4}$
e_2	$-1.051975059038994 \times 10^{-3}$
e_3	$8.314550749680474 \times 10^{-4}$
e_4	-0.263449668027011
e_5	$-5.756179604769289 \times 10^{-2}$
e_6	$-2.625043151678408 \times 10^{-5}$
e_7	$8.203467627872130 \times 10^{-5}$
e_8	$-2.206233257841825 \times 10^{-5}$
e_9	$1.610246501293106 \times 10^{-2}$
e_{10}	$3.517633816676780 \times 10^{-3}$
e_{11}	$7.659997874532446 \times 10^{-8}$
e_{12}	$-6.950614544672141 \times 10^{-7}$
e_{13}	$-4.359390762535273 \times 10^{-8}$
e_{14}	$-2.926823382923164 \times 10^{-4}$
e_{15}	$-6.396214546640412 \times 10^{-5}$
e_{16}	$1.290199629163741 \times 10^{-9}$
e_{17}	$5.977694565243003 \times 10^{-10}$
e_{18}	$2.045156412928934 \times 10^{-9}$
e_{19}	$1.625620924811126 \times 10^{-6}$
e_{20}	$3.553691310366128 \times 10^{-7}$

comparison that can be made is between a dipolar and a quadrupolar model which both have the same Boyle temperature. For $L^* = 1$, the dipolar model with $(\mu^*)^2 = 6$ has practically the same T_B^* as the quadrupolar model with $(Q^*)^2 = 4$. In Fig. 4 results for B_2 for these two models are presented. As can be seen the dipolar model has the lower value of the second virial coefficient.

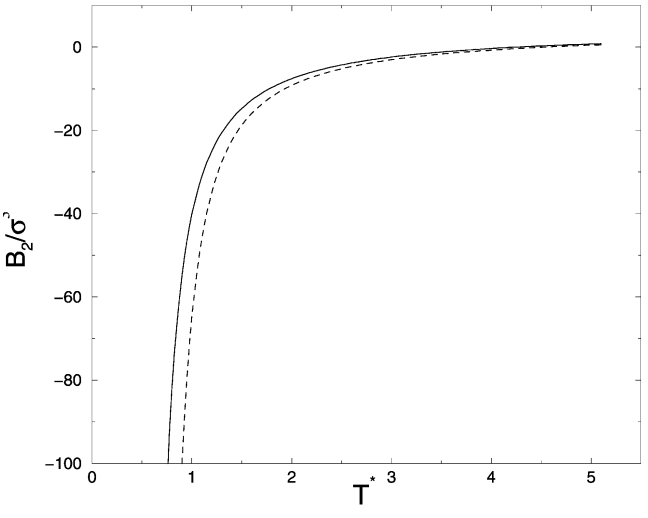

Fig. 3 Reduced second virial coefficient for models with $L^* = 1$. Results for a dipolar model with $(\mu^*)^2 = 4$ and $\alpha = 0$ (solid line) and a quadrupolar model with $(Q^*)^2 = 4$ (dashed line).

An interesting property is the ratio of the T_B/T_c, where T_c is the critical temperature. This ratio has been analyzed in detail for several spherical fluids by several groups.[35,36] For a spherical LJ fluid this ratio is 2.6. In Table 4 this ratio is presented for several quadrupolar and dipolar fluids. For $L^* = 0$ critical properties were taken from simulations results of refs. 37–40. For 2CLJQ and 2CLJD models critical properties were taken from refs. 34 and 33 respectively.

The ratio of T_B/T_c obeys the following rules. For non-polar models the ratio T_B/T_c decreases as the reduced bond length increases. For quadrupolar models (2CLJQ) with a given reduced bond length L^* the ratio T_B/T_c decreases as the quadrupole moment $(Q^*)^2$ increases. This reduction is more pronounced as the molecule becomes more spherical (*i.e.* as L^* becomes smaller). For dipolar fluids (2CLJD) with a given reduced bond length the ratio T_B/T_c decreases for moderate values of the dipole moment, reaches a minimum and then increases as the dipole moment increases. The effect of the dipole moment on T_B/T_c is much smaller than the effect of the quadrupole moment on this ratio. As can be seen the ratio T_B/T_c decreases as the anisotropy of the intermolecular forces increases (except for high dipole moments where this trend is inverted). The anisotropy of the intermolecular forces increases with the molecular elongation L^* and with the polar forces (*i.e.* quadrupolar or dipolar). Therefore one may suspect that the ratio T_B/T_c decreases as the acentric factor, ω, increases. This idea has been recently proposed by Iglesias-Silva and Hall.[41]

In the following section the results of this work are used to describe the second virial coefficient of real substances.

IV. Application to real substances

The purpose of this section is to use the results of the previous section to describe B_2 for real substances. Our goal is not to provide an extensive test of the performance of the 2CLJD in describing B_2 for real substances, but rather to provide a few illustrative examples.

It would be interesting to have an empirical expression for B_2 as a function of T^*, α, $(\mu^*)^2$ and L^*. This would allow one to use values of α, $(\mu^*)^2$ and L^* different from those used in this work (say for instance $L^* = 0.43$, $\alpha = 20$, and $(\mu^*)^2 = 3.47$). In view of this an effort was made to obtain a fit, using up to 50 parameters. However, the results were not satisfactory since the deviation between the tabular data generated in the previous section and the empirical fit was significant. For that reason we decided to use the tabular data generated in the previous section to describe real substances.

Therefore the question is the following: given a certain model, (*i.e.* a value of L^*, α and $(\mu^*)^2$), along with a list of B_2^* for many reduced temperatures T^*, which values of ε and σ best reproduce the experimental results of B_2? Notice that the conversion from reduced units to experimental units can be easily performed given

$$T/\mathrm{K} = T^*(\varepsilon/k) \tag{8}$$

$$B_2/\mathrm{cm}^3\ \mathrm{mol}^{-1} = 0.6023\ B_2^*\sigma^3 \tag{9}$$

where σ is given in Å and (ε/k) is given in K. Refrigerants are good candidates to be modeled using the 2CLJD model. Most refrigerants are halogenated derivatives of methane and ethane and for these the 2CLJD appears a reasonable model. Moreover they are substances of high technological interest and as such their virial coefficients have been studied in great detail.[42] Three substances have been selected, namely CH_3Cl, CH_3CHF_2 and CH_3CH_2Cl. The experimental values of the

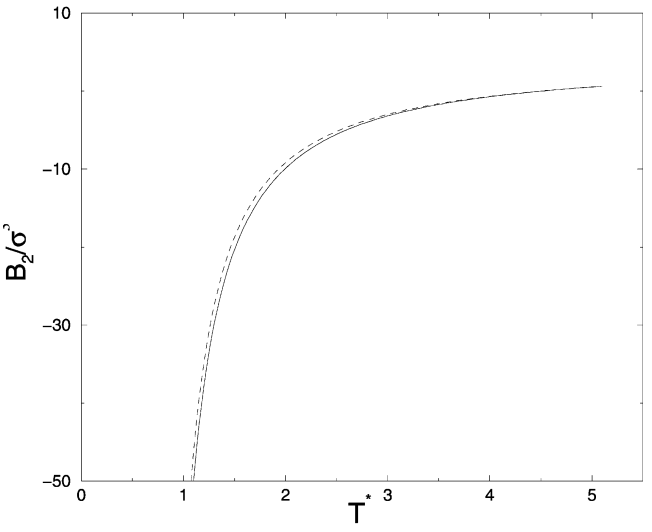

Fig. 4 Reduced second virial coefficient for models with $L^* = 1$. Results for a dipolar model with $(\mu^*)^2 = 6$ and $\alpha = 0$ (solid line) and a quadrupolar model with $(Q^*)^2 = 4$ (dashed line). Both models have the same Boyle temperature.

second virial coefficient for these three substances were taken from the compilation of Dymond and Smith.[43] For each substance the highest and lowest temperatures considered correspond to the highest and lowest temperatures included in the compilation. For each model we determine the values of σ and ε that minimize the deviation with respect to the experimental results, *i.e.* we minimize the function

$$\Phi = \sum \left(B_2^{\text{cal}} - B_2^{\text{exp}}\right)^2. \tag{10}$$

When the second virial coefficient of a certain model was required at a reduced temperature that was not available in our tables, we used a linear interpolation procedure. Since the number of temperatures for which B_2 is available for each model is of the order of 300, we believe that this interpolation procedure results in an acceptably small error. The FORTRAN program that allows one to choose the model that best describes a certain experimental data set is available upon request and as ESI.†

Table 4 Ratio of the Boyle and the critical temperature, T_B/T_c, for several polar models. Boyle temperatures for 2CLJD as obtained in this work. Boyle temperatures for 2CLJQ as reported in our previous work.[19] The critical temperatures of the 2CLJQ and 2CLJD models were obtained from computer simulations as reported in refs. 33,34,37–40

Quadrupolar models				
L^*	$(Q^*)^2$	T_c	T_B	T_B/T_c
0	0	1.31	3.42	2.61
0	1	1.60	3.78	2.36
0	2	2.25	4.70	2.09
0.6	0	2.45	5.85	2.39
0.6	2	2.58	6.00	2.32
0.6	4	2.87	6.34	2.21
Dipolar models				
L^*	$(\mu^*)^2$	T_c	T_B	T_B/T_c
0	0	1.31	3.42	2.61
0	2	1.61	4.01	2.49
0	4	2.07	5.32	2.57
0	6	2.55	6.93	2.71
0.505	0	2.71	6.66	2.46
0.505	2	2.75	6.77	2.46
0.505	4	2.91	7.05	2.42
0.505	8	3.27	8.09	2.47

In Table 5 we present the root mean square deviation between experimental and calculated values of B_2 for different substances along with the parameters that best describe the experimental results (for each elongation). Four elongations have been considered, namely $L^* = 0$, 0.4, 0.5, 0.6. The following conclusions can be obtained from the results of Table 5. The second virial coefficient of the three refrigerants considered can be satisfactory described by the 2CLJD model. The deviation between experimental and calculated values is only slightly larger than the experimental uncertainty. The Stockmayer potential (*i.e.* $L^* = 0$) reproduces the second virial coefficients as well as the models with non-zero values of L^*. This is somewhat surprising since the refrigerants considered are certainly non-spherical. The 2CLJD model with non-zero values of L^* performs better than a spherical dipolar model when it comes to reproducing liquid state properties.[26] More realistic models of refrigerants are certainly non-spherical.[44] In Table 5 we have also included the values of the dipole moment and the molecular volume which were obtained using "optimum" parameters. One may convert from reduced dipole moment to the dipole moment (in debye) using the formula:

$$\mu/\text{D} = \sqrt{\frac{(\mu^*)^2(\varepsilon/k)(\sigma^3)}{7243.3364}}. \tag{11}$$

The molecular volume of the molecule can be approximated to that of a hard dumbbell with a reduced bond length L^* and diameter σ using

$$V_m = \frac{\pi}{6}\sigma^3\left(1 + 1.5\ L^* - \frac{1}{2}(L^*)^3\right). \tag{12}$$

Note that in eqn. (12) the volume V_m does not account for the 'excluded' volume. In Table 5 the experimental values of the dipole moment are also included. As can be seen the value of the dipole moment that results from the "optimum" parameters does not agree with the experimental value of the dipole moment.[30,45,46] Also notice that the molecular volume of the different "optimum" parameters differs significantly. The message from Table 5 is the following. It is possible to perform a reasonably good fit to the second virial coefficient of real dipolar substances. However, if the only criterion for determining the potential parameters is the minimization of the difference between experimental and theoretical results, then the resulting

Table 5 Results for the second virial coefficient of real substances as described by the 2CLJD model. For each elongation, we present the model (*i.e.* the value of α and $(\mu^*)^2$) that best describes the experimental values of B_2. For this model the root mean square deviation (s) between experimental and calculated values is shown, expressed in $cm^3\ mol^{-1}$. The value of ε/k (in K) and σ (in Å) used in the calculations is shown. The first to the last column corresponds to the dipole moment (in D) as obtained from the calculation and that from experiment (in parenthesis). Finally the molecular volume of the model V_m (in $Å^3$) as given by eqn. (12) of the main text is presented

L^*	α	$(\mu^*)^2$	s	σ	ε	Dipole moment	V_m
CH_3–Cl							
0.0	0	3	7.83	4.10	215	2.47(1.87)	36.08
0.4	60	8	7.58	3.86	93	2.43(1.87)	47.22
0.5	60	6	7.45	3.68	121	2.23(1.87)	44.03
0.6	30	8	7.72	3.54	124	2.46(1.87)	41.62
CH_3CHF_2							
0	0	6	9.18	4.59	118	3.08(2.27)	50.96
0.4	60	10	9.52	3.86	87	2.62(2.27)	47.21
0.5	60	10	9.18	4.13	85	2.88(2.27)	62.69
0.6	30	10	9.48	3.44	120	2.60(2.27)	38.19
CH_3CH_2Cl							
0	0	6	11.28	4.24	148	3.05(2.05)	39.91
0.4	90	10	11.42	3.96	94	2.83(2.05)	50.98
0.5	60	10	11.47	3.88	105	2.91(2.05)	51.61
0.6	30	10	11.42	3.28	146	2.67(2.05)	33.10

parameters lack any physical meaning, the dipole moment can deviate significantly from the experimental value and the molecular volume can be quite different from that obtained from physical considerations. The second virial coefficient certainly depends on the pair potential between molecules, but it is not sensitive enough to discriminate between different molecular models.

In our view a much better approach to the problem is the following. One can, for example, impose a molecular volume from physical considerations. Thus for a given value of L^* the value of σ must be chosen to reproduce the molecular volume using eqn. (12). Once the value of σ is fixed from the molecular volume, one performs the optimization with respect to ε in order to minimize the deviation with respect to the experimental results.

Approximate molecular volumes can be obtained from experimental vapor pressure molar volumes using a one center Lennard-Jones model (see refs. 27,47 for details). However, we shall adopt the following, somewhat simpler approach; the volume of CH_3CHF_2 as taken from liquid state simulations is approximately 50 $Å^3$.[26] We shall therefore adopt this volume for CH_3CHF_2. The volume of CH_3CH_2Cl should be somewhat larger, and that of CH_3Cl somewhat smaller. For simplicity we shall simply assume that the volume of the three substances is of the order of 50 $Å^3$, which is qualitatively correct. The parameters obtained by imposing this molecular volume are presented in Table 6.

The goodness of the fit as given by the root mean square deviation are also presented. In Fig. 5, Fig. 6 and Fig. 7 the second virial coefficient for CH_3Cl, CH_3CHF_2 and CH_3CH_2Cl are presented. Experimental results and those of the calculations are presented. The model used in those figures for each substance is that presented in bold in Table 6. Although the fit to the data of Table 6 is slightly worse than that presented in Table 5 the advantage of the procedure is that the potential parameters are now much more realistic. Moreover it is now seen that when a reasonable value of the molecular volume is imposed then an anisotropic model better describes the

Table 6 As in Table 5, but when the molecular volume is fixed to 50 $Å^3$. In this case σ is not adjusted but is obtained from eqn. (12) of the main text. Therefore in this table the only parameter that was fitted to reproduce the experimental results of B_2 is ε. In bold are shown the models used to compare with the experimental results in Figs. 5–7

L^*	α	$(\mu^*)^2$	s	σ	ε	Dipole	V_m
CH_3–Cl							
0	0	3	10.17	4.57	191	2.75(1.87)	50
0.4	**60**	**8**	**7.57**	**3.93**	**91**	**2.47(1.87)**	**50**
0.5	90	6	8.18	3.84	111	2.28(1.87)	50
0.6	60	6	8.58	3.76	123	2.33(1.87)	50
CH_3CHF_2							
0	0	6	10.19	4.57	119	3.06(2.27)	50
0.4	90	8	10.84	3.93	95	2.52(2.27)	50
0.5	**60**	**8**	**11.21**	**3.84**	**106**	**2.57(2.27)**	**50**
0.6	90	6	13.60	3.76	127	2.37(2.27)	50
CH_3CH_2Cl							
0	0	6	13.71	4.57	138	3.30(2.05)	50
0.4	90	10	14.09	3.93	95	2.83(2.05)	50
0.5	**60**	**10**	**11.59**	**3.84**	**106**	**2.88(2.05)**	**50**
0.6	60	8	11.88	3.76	130	2.76(2.05)	50

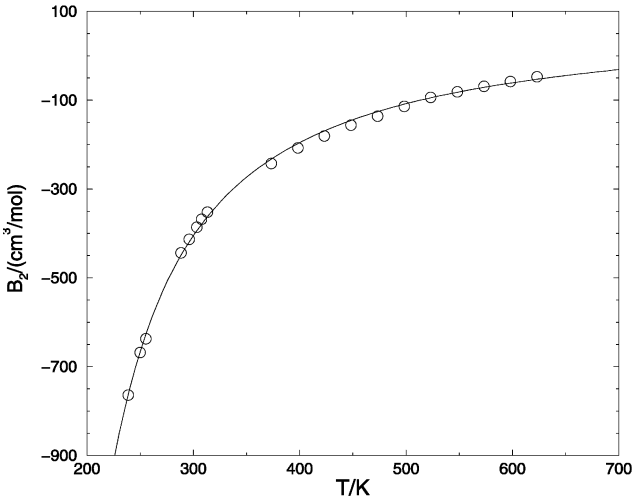

Fig. 5 Second virial coefficient of CH_3Cl as obtained from experiment (symbols)[43] and from the calculations of this work for the 2CLJD (solid line). The parameters used to describe CH_3Cl with the 2CLJD model are those presented in bold for CH_3Cl in Table 6.

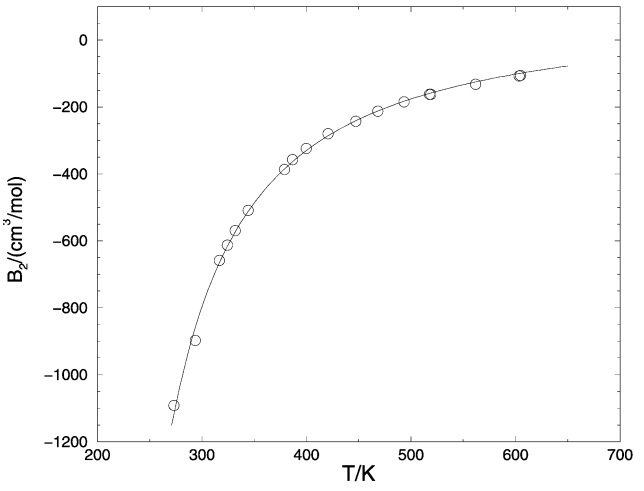

Fig. 7 Second virial coefficient of CH_3CH_2Cl as obtained from experiment (symbols)[43] and from the calculations of this work for the 2CLJD (solid line). The parameters used to describe CH_3CH_2Cl with the 2CLJD model are those presented in bold for CH_3CH_2Cl in Table 6.

experimental results (the only exception being the CH_3-CHF_2). The dipole moments obtained from our calculations tend to be 20% larger than the experimental values. We do not have an explanation for this; there may be a number of contributing factors. For example the lack of molecular polarisability in the model could account for around a quarter of this discrepancy. The inclusion of molecular polarisability has been proved to be important when dealing with dipolar molecules in the liquid phase,[48] though slightly less so for the gas phase. Also, as mentioned earlier, an ideal dipole is only an approximation to the actual interaction energy between two charge distributions.

In summary the 2CLJD model provides a good description of the second virial coefficient of the three refrigerants considered. The typical deviations between experimental and calculated values of B_2, as given by the root mean square deviation, is similar to those obtained by empirical correlations (see the work by Tsonopoulos[49] and for an application to refrigerants see the work by Dymond[42]).

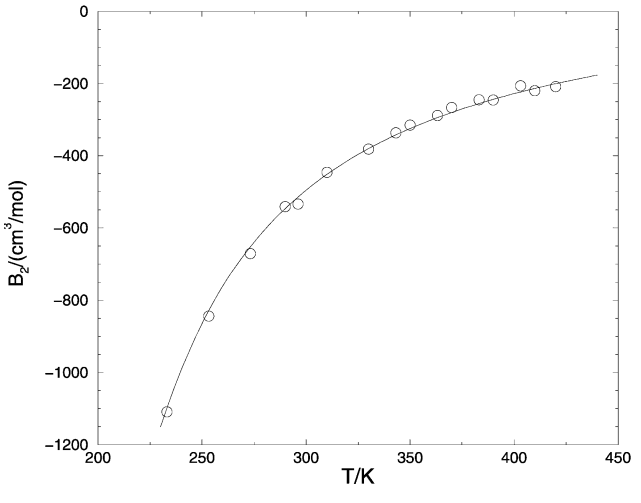

Fig. 6 Second virial coefficient of CH_3CHF_2 as obtained from experiment (symbols)[43] and from the calculations of this work for the 2CLJD (solid line). The parameters used to describe CH_3CHF_2 with the 2CLJD model are those presented in bold for CH_3CHF_2 in Table 6.

V. Conclusions

In this paper the second virial coefficient has been calculated for a number of two-center LJ models with a point dipole moment. A number of elongations, reduced dipole moments, and angles between the dipole moment and the molecular axis were considered. For each model the reduced second virial coefficient and the Boyle temperature were determined. All results are available in electronic format as ESI.† The data set of the Boyle temperature was fitted to an empirical expression.

The presence of the dipole moment reduces the second virial coefficient with respect to that of the non-polar model. The dipole also increases the value of the Boyle temperature. The effect is more pronounced for a certain reduced dipole, when the dipole moment forms an angle to the molecular axis. Thus a non-axial dipolar moment has a "similar" effect to that of a larger axial dipole moment. For a certain reduced multipolar moment, the quadrupole is more effective than the dipole in reducing B_2. The value of T_B/T_c decreases with L^* and with the presence of polar forces (quadrupolar or dipolar). At large values of the dipole moment this trend is inverted.

We have shown how the data in this work can be used in the determination of potential parameters for the pair potential with a view to reproducing B_2 for real substances. A first approach allowing the parameters full freedom yields, in general, a reasonable fit, however the parameters lack any physical meaning. This was illustrated in Table 5. A more reasonable approach is to impose a value of the molecular volume (as well as perhaps that of L^*) from physical grounds and optimize only the value of ε, as was shown in Table 6. When this is done it is seen that the inclusion of molecular anisotropy improves the description of real substances. However, it is worth reiterating the idealized character of the 2CLJD model. As mentioned earlier true dipolar molecules are heteronuclear rather than homonuclear. Also, real dipolar molecules can be polarized by a polar molecule, an effect that has been neglected in this work. The ideal dipole is also an ideal description of the coulombic interaction energy between two charge distributions. In fact, a model with two partial charges located in each of the sites of the 2CLJ model could yield a better description and has been considered previously in theoretical and simulation work.[50,51]

We hope the data obtained in this work can be useful for workers wishing to describe experimental results for B_2 for real

substances with the 2CLJD model. An area of particular interest is that of refrigerants. Refrigerants are usually ethane derivates, thus the 2CLJD model represents a reasonable first approximation. Also, workers looking for potential parameters to describe liquid properties can make use of this, and similar, studies. It is possible to proceed in a two step approach in the search of a potential parameter set. First, determine a set of potential parameters describing the gas phase (*i.e.* the second virial coefficient) and then proceed to a refinement of the parameters by means of computer simulations in the liquid phase. This approach has been used successfully for n-alkanes.[52] It should be stated that parameters describing gas phase properties are not generally transferable to the liquid phase and vice versa. It should be mentioned that three body forces play an important role in determining liquid phase properties, whereas they have a diminished role in the gas phase. Therefore, potential parameters determined for the liquid phase can be considered as effective potential parameters rather than the true pair potential parameters. In any case, having a reasonable potential parameter set correctly describing the second virial coefficient is a great help, since usually a minor modification of the model (typically decreasing ε by a 10%) yields a reasonable model for the liquid phase.

Along with this work the second virial coefficient of 2CLJ, 2CLJQ and 2CLJD models is now available. Some future areas of interest would be the determination of the third virial coefficient for these models. For example a comprehensive study of the third virial coefficient for the non-polar 2CLJ model is yet to be undertaken (a small number of data points have been reported in ref. 53).

Acknowledgement

Financial support is due to project number BFM-2001-1420-C02-01 of the Spanish DGICYT (Dirección General de Investigación Científica y Técnica). One of the authors, C. McBride, would like to acknowledge and thank the European Union FP5 Program for the award of a Marie Curie post-doctoral fellowship (No. HPMF-CT-1999-00163).

We would like to thank Dr Duarte for bringing ref. 5 to our attention which was overlooked in ref. 19. The experimental values of the second virial coefficient of xenon + ethane and xenon + ethene reported in the work of ref. 19 were taken from ref. 5.

References

1 A. A. Fredenslund, J. Mollerup and L. J. Christiansen, *Cryogenics*, 1973, **13**, 414.
2 F. Fontalba, K. N. Marsh, J. C. Holste and K. R. Hall, *Fluid Phase Equilib.*, 1988, **41**, 141.
3 A. A. Ricardo and M. N. da Ponte, *J. Phys. Chem.*, 1996, **100**, 18 839.
4 A. A. Ricardo, M. N. da Ponte and J. Fischer, *J. Phys. Chem.*, 1996, **100**, 18 844.
5 C. M. M. Duarte, *Comportamento (pVTx) de misturas de xenon + etano e xenon + eteno. Segundo e terceiro coeficientes do virial.*, PhD Thesis, Lisbon, 1997.
6 J. E. Mayer, *J. Chem. Phys.*, 1937, **5**, 67.
7 J. E. Mayer, *J. Phys. Chem.*, 1939, **43**, 71.
8 J. E. Mayer and M. G. Mayer, *Statistical Mechanics*, John Wiley and Sons Inc., New York, 1940.
9 J. O. Hirschfelder, C. F. Curtiss and R. B. Bird, *Molecular Theory of Gases and Liquids*, John Wiley, New York, 1954.
10 D. A. McQuarrie, *Statistical Mechanics*, Harper and Row, New York, 1976.
11 J. P. Hansen and I. R. McDonald, *Theory of Simple Liquids*, Academic Press, London, 1986.
12 J. E. Lennard-Jones, *Proc. R. Soc. London, Ser. A*, 1924, **106**, 463.
13 J. E. Lennard-Jones, *Proc. Phys. Soc. London*, 1931, **A43**, 461.
14 T. Boublik and I. Nezbeda, *Coll. Czech. Chem. Commun.*, 1986, **51**, 2301.
15 T. Kihara, *Intermolecular Forces*, John Wiley and Sons, Bath, 1978.
16 C. Vega and D. Frenkel, *Mol. Phys.*, 1989, **67**, 633.
17 G. C. Maitland, M. Rigby, E. B. Smith and W. A. Wakeham, *Intermolecular forces, their origin and determination*, Clarendon Press, Oxford, 1981.
18 T. Boublik, *Coll. Czech. Chem. Commun.*, 1994, **59**, 756.
19 C. Menduina, C. McBride and C. Vega, *Phys. Chem. Chem. Phys.*, 2001, **3**, 1289.
20 W. H. Stockmayer, *J. Chem. Phys.*, 1941, **9**, 398.
21 J. S. Rowlinson, *Trans. Faraday Soc.*, 1949, **45**, 974.
22 J. S. Rowlinson, *J. Chem. Phys.*, 1951, **19**, 827.
23 J. M. Prausnitz, R. N. Lichtenthaler and E. G. de Azevedo, *Molecular Thermodynamics of Fluid Phase Equilibria*, Prentice Hall, White Plains, 1999.
24 R. F. Blanks and J. M. Prausnitz, *AIChE J.*, 1962, **8**, 86.
25 W. Ameling, K. P. Shukla and K. Lucas, *Mol. Phys.*, 1986, **58**, 381.
26 C. Vega, B. Saager and J. Fischer, *Mol. Phys.*, 1989, **68**, 1079.
27 F. Kohler and N. van Nhu, *Mol. Phys.*, 1993, **80**, 795.
28 H. Conroy, *J. Chem. Phys.*, 1967, **47**, 5307.
29 I. Nezbeda, J. Kolafa and S. Labik, *Czech. J. Phys.*, 1989, **B39**, 65.
30 C. G. Gray and K. E. Gubbins, *Theory of molecular fluids*, Clarendon Press, Oxford, 1984.
31 W. H. Keesom, *Comm. Phys. Lab. Leiden*, 1912, Suppl. 24b).
32 W. H. Keesom, *Comm. Phys. Lab. Leiden*, 1915, Suppl. 39a).
33 M. Lisal, R. Budinsky and V. Vacek, *Fluid Phase Equilib.*, 1997, **135**, 193.
34 J. Stoll, J. Vrabec, H. Hasse and J. Fischer, *Fluid Phase Equilib.*, 2001, **179**, 339.
35 G. A. Vliegenthart and H. N. W. Lekkerkerker, *J. Chem. Phys.*, 2000, **112**, 5364.
36 M. G. Noro and D. Frenkel, *J. Chem. Phys.*, 2000, **113**, 2941.
37 M. E. Van-Leeuwen, B. Smit and E. M. Hendriks, *Mol. Phys.*, 1993, **78**, 271.
38 B. Garzon, S. Lago and C. Vega, *Chem. Phys. Lett.*, 1994, **231**, 366.
39 B. Smit and C. P. Williams, *J. Phys. Condens. Matter*, 1990, **2**, 4281.
40 M. R. Stapleton, D. J. Tildesley, A. Z. Panagiotopoulos and N. Quirke, *Mol. Simul.*, 1989, **2**, 147.
41 G. A. Iglesias-Silva and K. R. Hall, *Ind. Eng. Chem. Res.*, 2001, **40**, 1968.
42 J. H. Dymond, *Fluid Phase Equilib.*, 2000, **174**, 13.
43 J. H. Dymond and E. B. Smith, *The virial coefficient of pure gases and mixtures*, Clarendon Press, Oxford, 1980.
44 M. Lisal and V. Vacek, *Mol. Phys.*, 1996, **87**, 167.
45 D. E. Stogryn and A. P. Stogryn, *Mol. Phys.*, 1966, **11**, 371.
46 R. C. Weast, *Handbook of Chemistry and Physics*, CRC, Boca Raton, 1986.
47 J. Fischer, R. Lustig, H. Breitenfelder-Manske and W. Lemming, *Mol. Phys.*, 1984, **52**, 485.
48 T. Boublik and J. Winkelmann, *Mol. Phys.*, 1999, **96**, 435.
49 C. Tsonopoulos, *AIChE J.*, 1974, **20**, 263.
50 M. Lupkowski and P. A. Monson, *Mol. Phys.*, 1989, **67**, 53.
51 G. S. Dubey, S. F. O'Shea and P. A. Monson, *Mol. Phys.*, 1993, **80**, 997.
52 A. L. Rodriguez, C. Vega and J. J. Freire, *J. Chem. Phys.*, 1999, **111**, 438.
53 B. Tomberli, S. Goldman and C. G. Gray, *Fluid Phase Equilib.*, 2001, **187**, 111.